17th World Conference on Earthquake Engineering, 17WCEE
Sendai, Japan - September 13th to 18th 2020

AN ENERGY BASED DESIGN AND ASSESSMENT FRAMEWORK FOR EARTHQUAKE SOIL STRUCTURE INTERACTING SYSTEMS

H. Yang[(1)], H. Wang[(2)], B. Jeremić[(3)]

[(1)] *Postdoctoral Researcher, University of California Davis, hhhyang@ucdavis.edu*
[(2)] *PhD Candidate, University of California Davis, hexwang@ucdavis.edu*
[(3)] *Professor, University of California Davis, jeremic@ucdavis.edu*

Abstract
Presented is an energy based design and assessment framework for earthquake soil structure interaction (ESSI) systems. Presented framework is based on analytic calculation of seismic energy input and dissipation within the ESSI system. All components of energy dissipation are accounted for, including material inelastic behavior damping, viscous damping, radiation damping and algorithmic/numerical energy dissipation. One the key components of the material inelastic damping is the proper modeling of plastic free energy, which ensures that the second law of thermodynamics is enforced. A practical ESSI model composed of a frame structure, underlying soil, and soil-foundation interface is used to illustrate proposed energy based analysis framework.

Keywords: Earthquake Soil Structure Interaction; Seismic Energy; Finite Element; Energy Based Design

1. Introduction

Energy based design (EBD) is becoming a popular approach in the design and assessment of soil structure interaction (SSI) systems. While the traditional force-based and displacement-based design concepts mostly focus on system's peak response, EBD accounts for loading history effect by tracking accumulated material damage and time-dependent system response [1]. This is particularly important in the case of earthquake loading, where structures experience cyclic loading and continuously being damaged.

In the past few decades, EBD has been widely used in studies of seismic performance of structural and SSI systems. In most publications, energy analysis was carried out for simplified single degree of freedom (SDOF) and multiple degree of freedom (MDOF) systems [2-7]. This simplification is partially caused by the limitation of numerical analysis techniques and computational power at the time. With the improvement in modeling and simulation approaches, modern EBD can be improved to a new level of accuracy and efficiency.

2. Propagation and Dissipation of Seismic Energy in SSI System

Fig. 1 illustrates the propagation and dissipation of seismic energy, from earthquake source to local site. Only a portion of the potential energy released at earthquake source reaches the local site of interest. The focus of this study is on the transformation of input mechanical energy within the local SSI system.

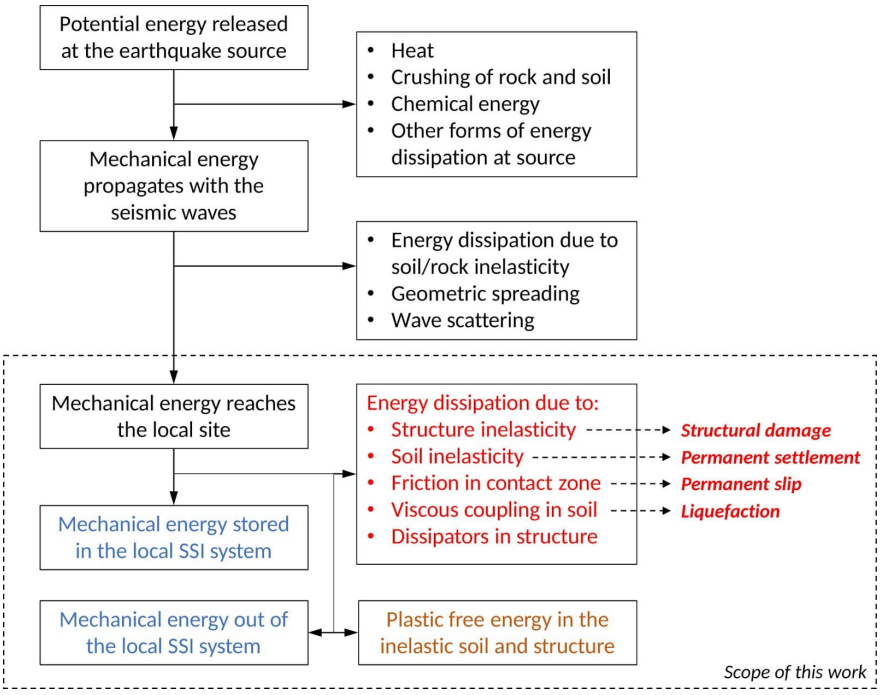

Fig. 1. Seismic energy propagation and dissipation, from source to local site.

For a SSI system under earthquake loading, as shown in Fig. 1, energy dissipation could be in the following forms:

- Material inelasticity/nonlinearity of soil;

- Material inelasticity/nonlinearity of structure;
- Frictional slipping in the contact interface zone between soil and foundation;
- Viscous coupling between pore water and soil skeleton in saturated or unsaturated soil;
- Viscous damping in the structural components;
- Material inelasticity or viscous damping in energy dissipators;
- Radiation of mechanical energy out of the local site (usually referred to as radiation damping).

In addition to the physical energy dissipation mechanisms, algorithmic damping, or numerical damping, should also be considered in numerical simulation of dynamic SSI systems. Yang et al. [8] pointed out that these energy dissipation mechanisms model fundamentally different physical or mathematical phenomena, and do lead to different system responses. It is important to model each energy dissipation mechanism by following proper physics and mathematics.

3. Modeling of Energy Dissipation in SSI System

When developing a numerical model for SSI system, each component is modeled using a different material constitutive model (sand, clay, rock, steel, concrete, isolator, damper, or other soil/structural materials). It is important to realize that each model is developed with its own assumptions and limitations. As a result, detailed energy computation approach varies for different material models and mechanisms.

One common misconception on energy dissipation due to material inelasticity is worth pointing out here. When an inelastic material yields and continues to be loaded, plastic deformation is developed. In many studies, all plastic deformation is assumed to lead to energy dissipation. However, it has been proven, experimentally and theoretically, that part of the plastic deformation leads to change in plastic free energy. Farren and Taylor [9] identified the role of plastic free energy and plastic energy dissipation in a series of experiments on metals and alloys. Since then, more work on this topic has been published [9-15].

Many of the commonly used soil models simply neglect plastic free energy, which leads to a common misconception about plastic work and plastic energy dissipation. Ziegler and Wehrli [9] derived constitutive relations for most popular soil models from free energy and dissipation function. Collins and Kelly [12] analyzed a family of soil models, including Mohr-Coulomb, original Cam clay, modified Cam clay, using the thermomechanical theory. Feigenbaum and Dafalias [13] presented a new interpretation of the pressure-independent, von Mises type material models under the thermomechanical framework. Yang et al. [15] proposed an energy dissipation computation approach for the pressure-dependent, Drucker-Prager plasticity models.

For the modeling of structural components, like beam-column and wall, nonlinear fiber section technique developed by Spacone et al. [16] is widely used. Concrete and steel are modeled as uniaxial fiber materials along the span of beam/column. The uniaxial steel model originally developed by Menegotto and Pinto [17] and later extended by Filippou et al. [18] is capable of capturing the nonlinear hysteretic behavior and isotropic strain-hardening effect of steel. Yassin [19] developed an uniaxial concrete material model based on the work of Kent and Park [20] and Scott et al. [21]. Yang et al. [22] developed formulations of plastic energy dissipation for the previously mentioned uniaxial structural material models.

Viscous damping is the result of dissipative interactions between solids and viscous fluids. Caughey damping [23], as well as its special case Rayleigh damping, is usually used to model viscous damping. As pointed out

by Hall [24], Rayleigh damping could cause unrealistically high damping forces, if the damping parameters are not chosen reasonably. Yang et al. [8] showed that unrealistic Rayleigh damping could easily overwhelm other energy dissipation mechanisms and lead to overconfidence in SSI system design.

Numerical damping does not represent any physical process but is used in time integration algorithms to achieve stable, converged simulation results. Newmark family algorithms [25-27] are the most commonly used time integration schemes. It should be mentioned that Newmark algorithm has been shown to have instability issues in certain cases [28]. And a few energy conserving time integration algorithms [28-31] were developed to mitigate this issue. Nonetheless, Newmark integration algorithm remains a popular choice and has proven to be reliable for finite element (FE) simulations within the scope of this work.

4. Numerical Example

The presented EBD analysis framework is implemented in the Real-ESSI Simulator System [32]. All aforementioned material models, elements, damping types, and solution schemes that are necessary for analyzing ESSI problems are available in Real-ESSI. The energy computation results can be directly visualized using ParaView [33] so that engineers can easily use this information to evaluate their designs. Detailed documentation of the code and more numerical examples can be found in Jeremić et al. [34].

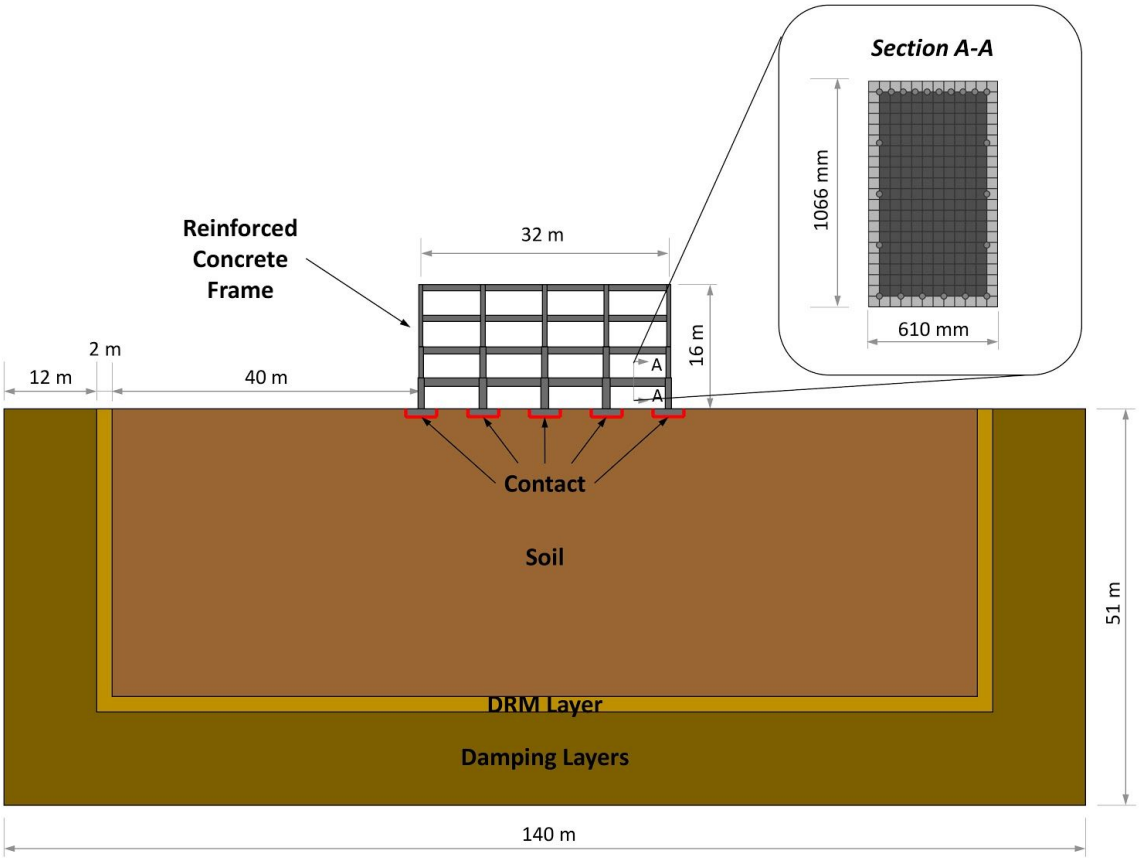

Fig. 2. Numerical model of the reinforced concrete frame, inelastic soil, and frictional interfaces.

An overview of the SSI model is shown in Fig. 2. The main components of the model include:

- A reinforced concrete frame modeled using beam-column elements, as well as the previously discussed steel and concrete fiber material models. The 4 story by 4 bay frame is modified after one of the code-conforming designs by Haselton et al. [35].
- The underlying soil modeled using regular 27-node-brick elements and Drucker-Prager inelastic material model with Armstrong-Frederick kinematic hardening.
- The interfaces between soil and foundation modeled using the nonlinear, stress-based, frictional slipping contact elements.
- A layer of DRM elements, for earthquake loading, modeled using 27-node-brick elements and linear elastic material.
- A few damping layers outside the DRM layer, to absorb the outgoing waves, also modeled using 27-node-brick elements and linear elastic material.

An inclined Ormsby wavelet motion is used in this study. Shown in Fig. 3 is the input Ormsby motion at earthquake source. The peak ground displacement at source is about 0.012 m, which will be amplified when reaching the local site. The angle of inclination is 15°, which is within the common range for realistic seismic motions. The motion has frequency contents between 1 Hz and 4 Hz, with a constant peak between 2 Hz and 3 Hz in frequency domain. Note that this frequency range covers the first and possibly the second eigenfrequency of the frame model.

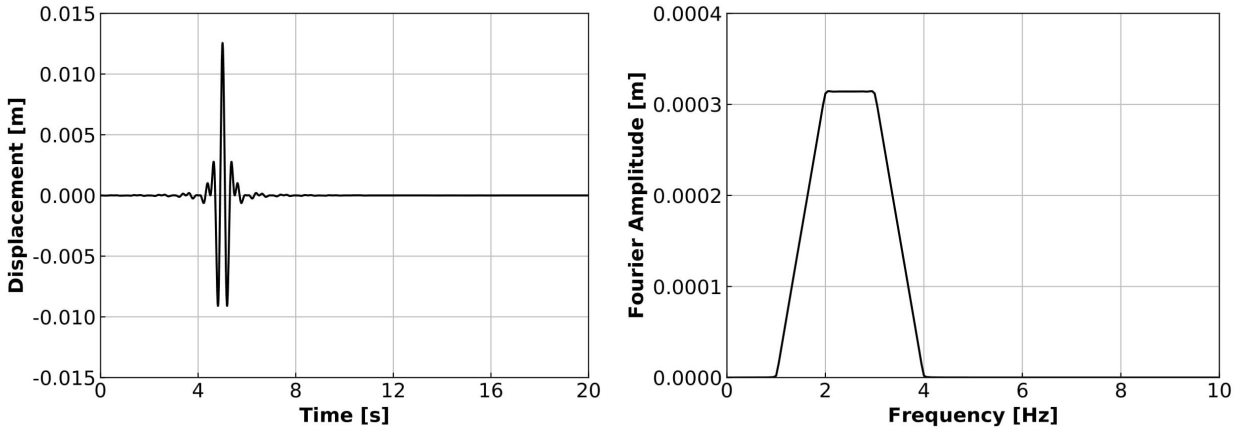

(a) Time history (b) FFT Spectrum

Fig. 3. Input Ormsby wavelet motion at earthquake source.

Fig. 4 presents the distribution of plastic energy dissipation evolving with time. Note that the interface elements between foundation and soil have zero volume, so small spheres are used to represent them in energy visualization. At t = 5 s shown in Fig. 4(a), before any significant motion reaches the frame, there is no plastic dissipation in the model. Then between t = 5 s and t = 8 s, plastic dissipation continuously accumulates in the frame, underlying soil, and soil-structure interface zones. Plastic dissipation in frame elements is concentrated around the connections between beams and columns. This is consistent with common knowledge on structural analysis. It is interesting to see that significant plastic dissipation is accumulated in the top two floor levels, while the lower floors see almost no dissipation.

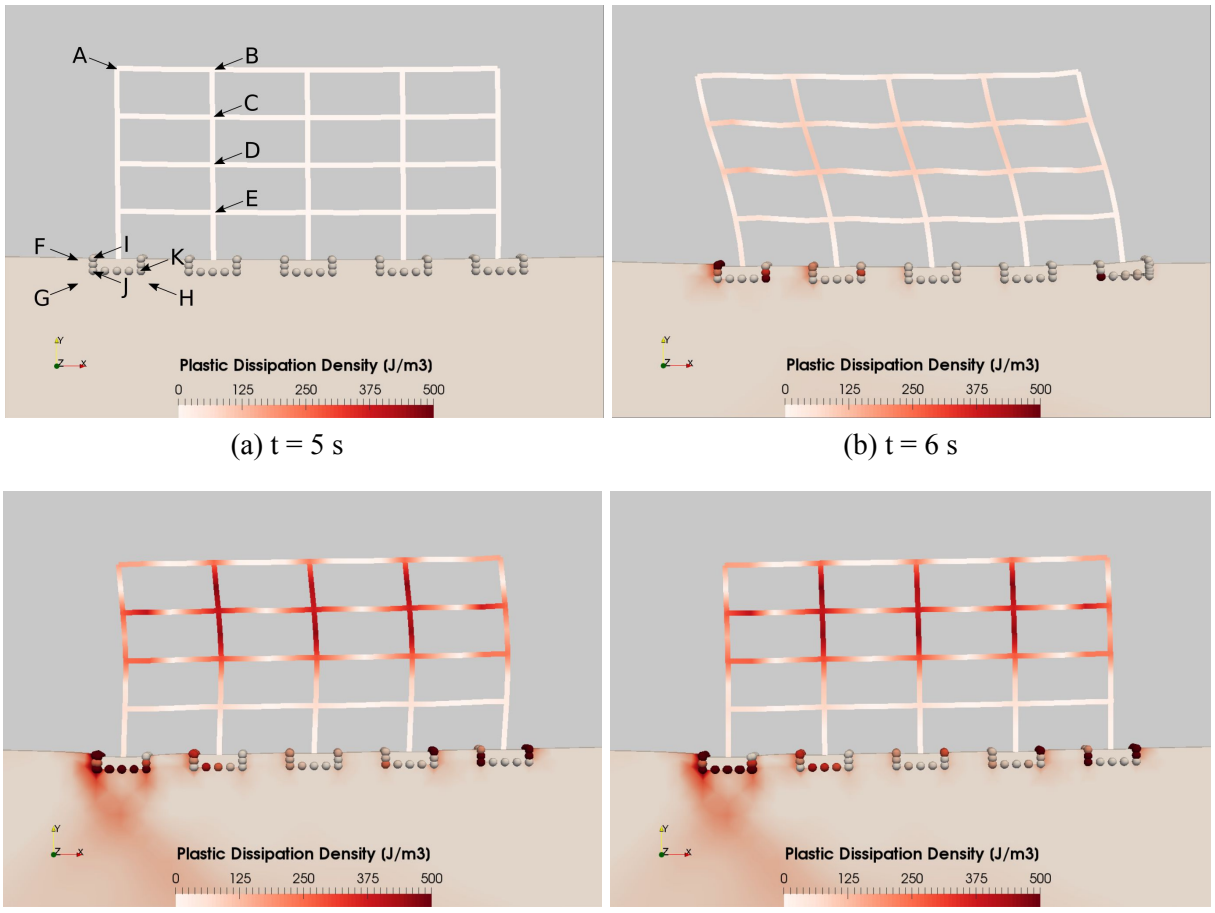

(a) t = 5 s (b) t = 6 s

(c) t = 7 s (d) t = 8 s

Fig. 4. Distribution of plastic energy dissipation evolving with time.

After identifying zones with large amounts of plastic dissipation, which indicates material damage, the next step is to investigate the accumulation of energy dissipation at specific locations. Fig. 5 shows the evolution of plastic dissipation density at the locations marked in Fig. 4 (a). For all locations, the rise of plastic dissipation happens at around t = 6 s, which is also when the peak displacement response is observed. Notice that the dissipation density at interface locations are two magnitudes larger than that at frame or soil locations. This is expected since the interface elements have much larger localized deformations, i.e. frictional slipping, that lead to highly concentrated energy dissipation.

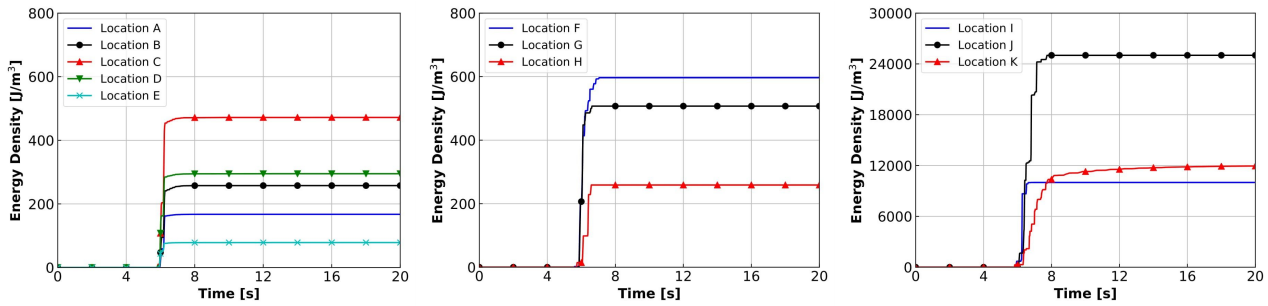

(a) Frame locations (b) Soil locations (c) Interface locations

Fig. 5. Evolution of plastic dissipation density at various locations.

5. Conclusions

Presented was an EBD framework for SSI system that was developed based on thermodynamics and engineering mechanics. Existing EBD approaches usually simplify realistic SSI system to MDOF, or even SDOF, model. The proposed EBD framework makes use of advanced modeling and simulation techniques so that the energy analysis provides more accurate and detailed information regarding system performance and safety.

In order to illustrate the proposed EBD framework, a practical SSI model composed of a frame structure, underlying soil, and soil-foundation interface was analyzed. Locations with high accumulated plastic dissipation were identified in frame, soil, and soil-foundation interface. Time histories of plastic dissipation density at various locations were also plotted. It was observed that, for every location, energy dissipation density had a sudden increase when the peak of input motion arrived at the frame. Using this example, it was illustrated that the proposed EBD framework is advantageous in following accumulated material damage and system performance during the entire loading history.

6. Acknowledgements

This work was supported in part by the US-DOE, by the University of California, and by a private donor.

References

[1] Papazafeiropoulos, G., Plevris, V., and Papadrakakis, M. (2017). "A new energy-based structural design optimization concept under seismic actions." Frontiers in Built Environment, 3, 44.

[2] Uang, C.-M. and Bertero, V. V. (1990). "Evaluation of seismic energy in structures." Earthquake Engineering & Structural Dynamics, 19(1), 77–90.

[3] Sucuoğlu, H. and Nurtuğ, A. (1995). "Earthquake ground motion characteristics and seismic energy dissipation." Earthquake engineering & structural dynamics, 24(9), 1195–1213.

[4] Manfredi, G. (2001). "Evaluation of seismic energy demand." Earthquake engineering & structural dynamics, 30(4), 485–499.

[5] Bojórquez, E., Reyes-Salazar, A., Terán-Gilmore, A., and Ruiz, S. (2010). "Energy-based damage index for steel structures." Steel and Composite Structures, 10(4), 331–348.

[6] Moustafa, A. (2011). "Damage-based design earthquake loads for single-degree-of-freedom inelastic structures." Journal of structural engineering, 137(3), 456–467.

[7] Mezgebo, M. G. and Lui, E. M. (2017). "A new methodology for energy-based seismic design of steel moment frames." Earthquake Engineering and Engineering Vibration, 16(1), 131–152.

[8] Yang, H., Wang, H., Feng, Y., Wang, F., and Jeremić, B. (2019c). "Energy dissipation in solids due to material inelasticity, viscous coupling, and algorithmic damping." ASCE Journal of Engineering Mechanics, 145(9).

[9] Ziegler, H. and Wehrli, C. (1987). "The derivation of constitutive relations from the free energy and the dissipation function." Advances in applied mechanics, 25, 183–238.

[10] Collins, I. F. and Houlsby, G. T. (1997). "Application of thermomechanical principles to the modelling of geotechnical materials." Proceedings of Royal Society London, 453, 1975–2001.

[11] Rosakis, P., Rosakis, A., Ravichandran, G., and Hodowany, J. (2000). "A thermodynamic internal variable model for the partition of plastic work into heat and stored energy in metals." Journal of the Mechanics and Physics of Solids, 48(3), 581–607.

[12] Collins, I. and Kelly, P. (2002). "A thermomechanical analysis of a family of soil models." Geotechnique, 52(7), 507–518.

[13] Feigenbaum, H. P. and Dafalias, Y. F. (2007). "Directional distortional hardening in metal plasticity within thermodynamics." International Journal of Solids and Structures, 44(22-23), 7526–7542.

[14] Yang, H., Sinha, S. K., Feng, Y., McCallen, D. B., and Jeremić, B. (2018). "Energy dissipation analysis of elastic-plastic materials." Computer Methods in Applied Mechanics and Engineering, 331, 309–326.

[15] Yang, H., Wang, H., Feng, Y., and Jeremić, B. (2019). "Plastic energy dissipation in pressure-dependent materials." ASCE Journal of Engineering Mechanics, 146(3), 04019139.

[16] Spacone, E., Filippou, F., and Taucer, F. (1996). "Fibre beam–column model for non–linear analysis of r/c frames 1. formulation." Earthquake Engineering and Structural Dynamics, 25, 711–725.

[17] Menegotto, M. and Pinto, P. E. (1973). "Method of analysis for cyclically loaded reinforced concrete plane frames including changes in geometry and non-elastic behaviour of elements under combined normal force and bending." Proceedings of IABSE Symposium, 15–22.

[18] Filippou, F. C., Bertero, V. V., and Popov, E. P. (1983). "Effects of bond deterioration on hysteretic behavior of reinforced concrete joints." Report no., Earthquake Engineering Research Center, University of California, Berkeley.

[19] Yassin, M. H. M. (1994). "Nonlinear analysis of prestressed concrete structures under monotonic and cyclic loads." Ph.D. thesis, University of California, Berkeley.

[20] Kent, D. and Park, R. (1971). "Flexural members with confined concrete." ASCE Journal of Structural Division, 97, 1969–1990.

[21] Scott, B., Park, R., and Priestley, M. (1982). "Fiber element modeling for seismic performance of bridge columns made of concrete-filled frp tubes." Journal of the American Concrete Institute, 79(1), 13–27.

[22] Yang, H., Feng, Y., Wang, H., & Jeremić, B. (2019). Energy dissipation analysis for inelastic reinforced concrete and steel beam-columns. Engineering Structures, 197, 109431.

[23] Caughey, T. (1960). "Classical normal modes in damped linear systems." ASME Journal of Applied Mechanics, 27, 269–271.

[24] Hall, J. F. (2006). "Problems encountered from the use (or misuse) of Rayleigh damping." Earthquake engineering & structural dynamics, 35(5), 525–545.

[25] Newmark, N. M. (1959). "A method of computation for structural dynamics." ASCE Journal of the Engineering Mechanics Division, 85, 67–94.

[26] Hilber, H. M., Hughes, T. J. R., and Taylor, R. L. (1977). "Improved numerical dissipation for time integration algorithms in structural dynamics." Earthquake Engineering and Structure Dynamics, 5(3), 283–292.

[27] Chung, J. and Hulbert, G. (1993). "A time integration algorithm for structural dynamics with improved numerical dissipation: the generalized-α method." Journal of applied mechanics, 60(2), 371–375.

[28] Krenk, S. (2014). "Global format for energy-momentum based time integration in nonlinear dynamics." International Journal for Numerical Methods in Engineering, 100(6), 458–476.

[29] Simo, J. C. and Wong, K. K. (1991). "Unconditionally stable algorithms for rigid body dynamics that exactly preserve energy and momentum." International journal for numerical methods in engineering, 31(1), 19–52.

[30] Bathe, K.-J. (2007). "Conserving energy and momentum in nonlinear dynamics: a simple implicit time integration scheme." Computers & structures, 85(7), 437–445.

[31] Gonzalez, O. (2000). "Exact energy and momentum conserving algorithms for general models in nonlinear elasticity." Computer Methods in Applied Mechanics and Engineering, 190(13-14), 1763–1783.

[32] Jeremic B, Jie G, Cheng Z, Tafazzoli N, Tasiopoulou P, Pisano F, Abell JA, Watanabe K, Feng Y, Sinha SK, Behbehani, F, Yang H, Wang H (1989-2019): The Real-ESSI Simulator System, University of California, Davis and Lawrence Berkeley National Laboratory. http://real-essi.info/.

[33] Ayachit, U. (2015). The ParaView Guide: A Parallel Visualization Application. Kitware, Inc., USA.

[34] Jeremic B, Yang Z, Cheng Z, Jie G, Tafazzoli N, Preisig M, Tasiopoulou P, Pisano F, Abell J, Watanabe K, Feng Y, Sinha SK, Behbehani F, Yang H, Wang H (1989-present): "Nonlinear Finite Elements: Modeling and Simulation of Earthquakes, Soils, Structures and their Interaction," Self Published, University of California, Davis, CA, USA, and Lawrence Berkeley National Laboratory, Berkeley, CA, USA. URL: http://sokocalo.engr.ucdavis.edu/~jeremic/LectureNotes/.

[35] Haselton, C. B., Goulet, C. A., Mitrani-Reiser, J., Beck, J. L., Deierlein, G. G., Porter, K. A., Stewart, J. P., and Taciroglu, E. (2008). "An assessment to benchmark the seismic performance of a code-conforming reinforced-concrete moment-frame building." Report No. 2007/1, Pacific Earthquake Engineering Research Center.

